Design of a Novel Mechatronic System to Test Prosthetic Feet Under Specific Walking Activity Loads and Evaluate their Lower Leg Trajectory Error

by

Heidi V. Peterson

B.S., Stanford University (2018)

Submitted to the Department of Mechanical Engineering
in partial fulfillment of the requirements for the degree of

Master of Science in Mechanical Engineering

at the

MASSACHUSETTS INSTITUTE OF TECHNOLOGY

September 2021

Author . . . .
Department of Mechanical Engineering
August 30, 2021

Certified by. . . . .
Amos G. Winter, V.
Associate Professor of Mechanical Engineering
Thesis Supervisor

Accepted by . . . .
Nicolas Hadjiconstantinou
Chairman, Department Committee on Graduate Theses

Design of a Novel Mechatronic System to Test Prosthetic Feet Under Specific Walking Activity Loads and Evaluate their Lower Leg Trajectory Error

by

Heidi V. Peterson

Submitted to the Department of Mechanical Engineering
on August 30, 2021, in partial fulfillment of the
requirements for the degree of
Master of Science in Mechanical Engineering

Abstract

Lower limb amputees, numbered at more than 40 million globally, are challenged with limited mobility due to prosthetic devices that do not fully restore the functionalities of their biological limbs. While commercially available energy storage and return feet do restore some of the functionalities of a missing limb, the development and use of these prosthetic devices are limited by the current design, evaluation, and prescription processes. This is because the connection between the combined mechanical characteristics of a foot and user outcomes, such as mobility, comfort, and walking effort, is not fully understood.

The lower leg trajectory error (LLTE) is a novel prosthetic foot performance metric that provides a quantitative connection between the mechanical characteristics of a foot and the expected gait of an amputee. Thus far, the LLTE value of a foot has only been calculated via simulation, which limits the practical use of the metric in prosthetic foot design, evaluation, and prescription. One way to systematically measure the LLTE value of a physical prosthetic foot would be through a mechanical bench test, but the capabilities of existing bench testing devices are insufficient due to limited degrees of actuation and reported accuracy.

The purpose of this work was to design the Prosthetic Foot Testing Device (PFTD), a mechatronic testing device that could apply specific and uncoupled GRFs to any CoP on a foot and measure its deflection, through which it could measure the LLTE value and thus predict walking performance of any passive prosthetic foot. First, we determined high-level functional requirements of the PFTD, including the ranges of reference loads and prosthetic foot deflections as well as the LLTE measurement accuracy, such that the PFTD could meaningfully measure the full range of commercially available prosthetic feet. Second, we derived the relationships between the variables used to calculate the LLTE metric and those controlled or measured by the PFTD. Third, we used these relationships to design the PFTD and perform sensitivity analysis to ensure it could meaningfully and accurately measure the LLTE value

of any passive prosthetic foot. In future work, the PFTD will be built, validated, and used to measure and compare the LLTE values of various prosthetic feet. The PFTD and theory presented herein may become a new tool in the prosthetics industry to systematically and amputee-independently measure and compare the performance of prosthetic devices using the LLTE value as a universal metric, which could ultimately improve the development and prescription processes of prostheses.

Thesis Supervisor: Amos G. Winter, V.
Title: Associate Professor of Mechanical Engineering

Acknowledgments

I would like to take the opportunity to thank several key individuals, without whom this accomplishment would not have been possible.

First and foremost, I would like to thank my advisor, Professor Amos Winter, for inviting me into the GEAR Lab and trusting me with this project. I am sincerely grateful for your support and guidance as this project morphed between its various forms. Your insight was invaluable as I addressed both engineering problems as well as general grad school challenges.

Next, I would like to thank Victor Prost for mentoring me on this project and providing his services as an all-knowing sounding board. You were a defining part of my grad school experience and I am extremely grateful. I would also like to thank the other members of the prosthetics team: Brett, Nina, Charlotte, and Grace (our honorary member) for your help and camaraderie. I am grateful to all the members of the GEAR Lab for welcoming me into the community and fostering a wonderful environment that celebrates fun and hard work (not to mention athletics) equally.

Thank you to all my friends outside of the GEAR Lab and MIT who have experienced the past two years alongside me and made them so memorable.

As always, I am thankful for my family and Tom, for providing me with unfailing support and continuous encouragement throughout my years of study and through the process of researching and writing this thesis.

Contents

List of Figures

9

List of Tables

Chapter 1

Introduction

1.1   Background and Motivation

Lower limb amputees, numbered at more than 40 million globally [49, 28], are challenged with limited mobility due to prosthetic devices that do not fully restore the functionalities of their biological limbs [9]. Prosthesis users commonly use energy storage and return (ESR) feet, which are passive elastic prosthetic feet that act as springs by storing elastic energy during a step and releasing it at the end to assist with forward propulsion. While commercially available ESR feet do restore some of the functionalities of a missing limb, the development and use of these prosthetic devices are limited by the current design, evaluation, and prescription processes [23, 33, 11, 12, 42, 14, 20, 48]. The traditional design process relies on experimental and empirical iterative design, rather than a quantitative and predictive design framework [23]. The most common prosthesis evaluation method is human-subject testing, which involves subjective elements and has high variability between and within subjects [12, 20, 48, 45]. Due to its empirical nature, the traditional prescription process, which is based on observation, can be subjective and nonrepeatable, with variability between prosthetists and within different trials of a single prosthetist [12, 42, 14]. In addition to being resource-intensive, these processes result in products that do not serve the full amputee population; women and children in particular face challenges finding prostheses that are well-suited to their body characteristics [37, 19].

These processes may all benefit from predictive, quantitative, and repeatable methods, which would decrease the time and money required to design, evaluate, and prescribe a wider range of prosthetic feet.

To better design and prescribe prosthetic devices, there has been a growing effort within the prosthetics industry to utilize evidence-based practices and amputee-independent metrics. A prosthetic foot is defined by several mechanical properties that indirectly affect performance but cannot individually predict user outcomes. To this end, recent research has aimed to understand the relationship between a prosthetic foot's mechanical characteristics and its user's biomechanics [23, 24, 22]. Specifically, these studies have examined the effect of individual mechanical properties, such as stiffness, damping, hysteresis, energy return, and roll-over shape, on locomotion. However, the connection between the combined mechanical characteristics of a foot and user outcomes, such as mobility, comfort, and walking effort, is not fully understood [12]. Therefore, there is no firm consensus about what design criteria are required to maximize specific user outcomes [23, 33, 11, 24, 22, 40]. The lack of a quantitative and predictive connection between the combined mechanical characteristics of a prosthetic foot and its user's walking performance limits the design, evaluation, and prescription processes.

1.2 Lower Leg Trajectory Error (LLTE)

The lower leg trajectory error (LLTE) [27, 26, 36, 25, 35, 18] is a novel prosthetic foot performance metric that provides a quantitative connection between the mechanical characteristics of a foot and the expected gait of an amputee. The LLTE value is a single-value metric that represents the deviation (i.e., error) throughout a step between the predicted prosthetic-side lower leg trajectory and a target lower leg trajectory. The LLTE metric is calculated in the following manner. First, a reference dataset of able-bodied kinetic (forces) and kinematic (motion) walking gait data is scaled to a specific user's body characteristics (mass, height, and foot length). For each instance of a step, the scaled reference load, consisting of a ground reaction force

(GRF) applied at a specific center of pressure (CoP), is applied to a prosthetic foot. Since the foot is quasi-static and elastic, the lower leg trajectory (consisting of knee position and shank orientation) can be calculated from the resulting deformed shape of the foot (Fig. 1-1). The LLTE is defined as:

$$\text{LLTE} = \left[\frac{1}{N} \sum_{n=1}^{N} \left\{ \left(\frac{x_{\text{knee},n}^{\text{model}} - x_{\text{knee},n}^{\text{ref}}}{L_{\text{lower leg}}} \right)^2 + \left(\frac{y_{\text{knee},n}^{\text{model}} - y_{\text{knee},n}^{\text{ref}}}{L_{\text{lower leg}}} \right)^2 \right. \right.$$
$$\left. \left. + \left(\frac{\theta_{\text{lower leg},n}^{\text{model}} - \theta_{\text{lower leg},n}^{\text{ref}}}{\text{atan}(\frac{L_{\text{lower leg}}}{L_{\text{foot}}})} \right)^2 \right\} \right]^{\frac{1}{2}}, \tag{1.1}$$

where the superscripts "model" and "ref" refer to the calculated and reference values, respectively. N refers to the total number of frames (time instances of a step) included in the calculation, with n indicating each individual frame. The knee coordinates, x_{knee} and y_{knee}, are normalized by the lower leg length, $L_{\text{lower leg}}$, and the lower leg orientation, $\theta_{\text{lower leg}}$, is normalized by the angle formed by the foot and lower leg, $\text{atan}(\frac{L_{\text{lower leg}}}{L_{\text{foot}}})$.

The LLTE design framework is based on the LLTE metric and facilitates the design of user-specific prostheses by enabling the systematic tuning of the mechanical properties of prosthetic feet (geometry and stiffness) to yield a desired biomechanical response [26]. The LLTE design framework uses the LLTE value as the optimization objective metric: varying the geometry and stiffness of a foot to minimize its LLTE value. This results in an LLTE-optimal foot design that enables the user to most closely replicate the target walking pattern [35, 34]. To provide physical intuition, the lower the LLTE value, the closer the prosthetic foot replicates the target lower leg trajectory; an LLTE value of zero would correspond to a perfect replication.

The LLTE metric has been clinically validated as a single-value objective capable of predicting the biomechanical behavior of prosthetic feet, and the design framework has been shown to produce prosthetic feet that enable close to able-bodied walking patterns with similar or improved walking benefits compared with standard carbon fiber ESR feet [35, 18, 34]. A gait study that explored the sensitivity of LLTE-optimal
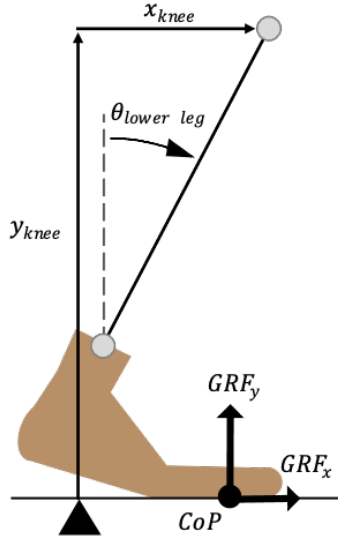
Figure 1-1: Schematic of the LLTE calculation conducted on the lower leg system in the sagittal plane. The position of the lower leg segment is defined by the horizontal and vertical positions of the knee (x_{knee} and y_{knee}), and the angle of the lower leg ($\theta_{\mathrm{lower\ leg}}$). Under prescribed loading conditions (GRF_{x}, GRF_{y}, and CoP), these coordinates, referred to as LLTE kinematic variables, can be calculated from the prosthetic foot deformation.

foot designs showed that the LLTE value of a prosthetic foot correlated to a user's ability to replicate a target walking pattern, preference, and clinical outcomes such as roll-over geometry, trunk sway, prosthetic energy return, and peak push-off power [34]. These studies validate the LLTE as a comprehensive amputee-independent metric that directly relates the mechanical properties of a foot to the walking performance of an amputee and has been shown to predict better (low LLTE value) or worse (high LLTE value) performance. Thus, we have chosen the LLTE value as the metric to use in this study.

Thus far, the LLTE value of a foot has only been calculated via simulation, which limits the practical use of the metric in prosthetic foot design, evaluation, and prescription. While finite element analysis (FEA) and modeling allow for relatively rapid testing and perfect replication of reference loads, the methods are limited by imperfect constitutive models of physical feet (especially so for certain manufacturing methods, such as 3D printing). Additionally, it is difficult to compare various commercially available feet because constitutive models either do not exist or are not

publicly available. It is not possible to measure the LLTE value of a foot via human-subject testing because a user will not necessarily apply the reference loads required to calculate the LLTE value.

1.3   Existing Prosthetic Testing Devices

One way to systematically measure the LLTE value of a physical prosthetic foot would be through a mechanical bench test, but the capabilities of existing bench testing devices are insufficient, due to limited degrees of actuation and reported accuracy. Existing devices have been designed to measure specific mechanical properties, such as strength and fatigue life [16, 17, 43]; stiffness and hysteresis [21, 3, 44, 1, 31]; damping [39]; viscoelasticity [10]; natural frequency [21]; energy return [44, 39, 32]; and roll-over shape [13, 6, 5]. To be able to measure the LLTE value of a foot, a device would require three degrees of actuation, so that it could apply horizontal and vertical GRFs at a specific CoP. Most existing devices are limited to one or two degrees of actuation, which prevents them from being able to apply specific walking loads and evaluate the response of the foot [16, 17, 21, 43, 3, 10, 1, 39, 13, 6, 5, 4, 31]. Several devices are actuated solely in the vertical direction, with the ability to manually choose a static incline angle (the angle between the foot and the simulated ground) [16, 21, 43, 3, 10, 1, 39, 13, 5], which prevents them from being able to vary the incline angle during a test. Other devices address this issue by actuating the incline angle as well as the vertical displacement [17, 6, 4], but are still unable to decouple the horizontal and vertical GRFs. This prevents the devices from being able to apply independent horizontal and vertical GRFs. In a study designed to test the stiffness and hysteresis properties of several prosthetic feet, Van Jaarsveld et al. [44] designed a measuring device with three degrees of actuation but only used the horizontal degree of actuation to prevent slippage between the foot and the simulated ground and did not report accuracy values of the device. In a study that used the same device to measure energy storage and release behavior of prosthetic feet, Postema et al. [32] proposed that the accuracy of the device may be insufficient. These limitations of

existing devices prevent them from being able to accurately measure the LLTE values of physical prosthetic feet.

1.4 Thesis Outline

This thesis builds upon earlier work done by Olesnavage K., Prost V., Johnson W., and Winter A. [27, 26, 36, 25, 35, 18]. The purpose of this work was to design the Prosthetic Foot Testing Device (PFTD), a mechatronic testing device that could apply specific and uncoupled GRFs to any CoP on a foot and measure its deflection, through which it could measure the LLTE value and thus predict walking performance of any passive prosthetic foot. The outline of the thesis is as follows:

Chapter 2: Definition of the Prosthetic Foot Testing Device functional requirements

This chapter discusses the process and rationale for determining high-level functional requirements of the PFTD. These included the ranges of reference loads and prosthetic foot deflections as well as the LLTE measurement accuracy, which were chosen to allow the PFTD to meaningfully measure the LLTE value of the full commercial range of prosthetic feet.

Chapter 3: Relationship between the lower leg trajectory error and the Prosthetic Foot Testing Device

The relationships between the variables used to calculate the LLTE metric and those controlled or measured by the PFTD are derived in this chapter. We investigate how these relationships were used to determine low-level functional requirements and perform sensitivity analysis to ensure the PFTD could accurately measure the LLTE value of any passive prosthetic foot.

Chapter 4: Machine design of the Prosthetic Foot Testing Device

This chapter explores the PFTD architecture and several key design choices that

were made to allow the PFTD to satisfy the functional requirements.

Chapter 5: Conclusion and future work

In conclusion, this chapter remarks on the importance of this work and provides an overview of future work.

Appendix: Additional considerations

Appendices provide more information about PFTD variable error sensitivities for all subject masses and stiffnesses as well as the inherited device design.

Chapter 2

Functional Requirements

The high-level functional requirements (Table 2.1) for the PFTD were set to allow it to evaluate the level ground walking performance of most commercially available passive prosthetic feet and achieve an accuracy similar to that of human perception. The most critical functional requirements for the PFTD include the ranges of reference loads and prosthetic foot deflections as well as the LLTE measurement accuracy.

2.1 Reference Loads and Prosthetic Foot Deflection Ranges

To understand the range of subject masses and activity levels that are served by existing commercially available feet, we examined previous comparative studies and commercially available prosthetic foot catalogs. The PFTD was designed to accommodate the full range of commercially available passive feet, which was determined by compiling the data from several prosthetic foot catalogs, which included brands such as Endolite, Fillauer, Freedom Innovations, Össur, and Ottobock [2, 8, 15, 29, 30]. Based on the data from these catalogs, the PFTD was designed to evaluate prosthetic feet with lengths up to 31 cm and heights ranging from 3.7 to 23.1 cm, and to apply able-bodied walking loads for users with body masses ranging from 40 to 200 kg. The ranges of GRFs (Table 2.1) that the PFTD must be able to apply to a foot were

Table 2.1: The high-level functional requirements of the PFTD.

Category	Requirement	Definition	Value/ Range [min, max]
Device Accuracy	LLTE Accuracy	The maximum error in LLTE value measurement	0.0059
LLTE Kinetic Variable Ranges	Range of GRF_x	The range of horizontal GRFs the PFTD must be able to apply to a foot	[-402.4 N, 408.7 N]
	Range of GRF_y	The range of vertical GRFs the PFTD must be able to apply to a foot	[49.48 N, 2,160 N]
LLTE Kinematic Variable Ranges	Range of x_knee	The range of horizontal positions of the knee the PFTD must enable	[-18.5 cm, 31.8 cm]
	Range of y_knee	The range of vertical positions of the knee the PFTD must enable	[42.3 cm, 53.9 cm]
	Range of θ_knee	The range of shank angles of the lower leg the PFTD must enable	[-21.6 deg, 39.3 deg]

calculated by scaling the loads from a target walking pattern by the range of subject masses. The target walking pattern was drawn from able-bodied level-ground walking data, published by D.A. Winter [47]. We chose able-bodied motion as the target walking pattern because many users want to replicate the symmetry and loading of able-bodied motion, there is no consensus on the ideal biomechanics of an amputee, and we have found in our work that even when the stiffness of a prosthetic foot is perturbed, amputees still approximate able-bodied motion [34]. The foot dimensions from the catalog data were used to determine certain PFTD dimensions as well as, in conjunction with the scaled dataset, to calculate the range of moments the PFTD must be able to withstand.

The prosthesis catalogs contained information about the range of subject masses but did not provide insight into the range of prosthetic foot stiffnesses within each subject mass category. Since the prosthesis catalogs did not report any measures of a foot's stiffness, the instantaneous stiffnesses of various prosthetic feet were calculated using data from a comparative study done by Webber and Kaufman [3, 46]. The study conducted the "Static Proof Test for Ankle-Foot Units" from ISO 10328 [16] on seven commercially available prosthetic feet, which were the same size and sourced for the same hypothetical subject, and then recorded their load-displacement curves. The feet were compared with two prototype LLTE-optimal feet that had been designed through the LLTE design framework as well as with an International Committee of the Red Cross (ICRC) Solid Ankle Cushion Heel (SACH) foot (Fig. 2-1), all of which were suitable for the hypothetical subject from Webber and Kaufman's study. The load-displacement curves of the LLTE-optimal and ICRC feet were measured according to the American Orthotics and Prosthetics Association (AOPA) "Dynamic Keel Test" procedure [3], which is similar to the protocol outlined in ISO 10328 [16]. The LLTE-optimal foot had been optimized through the LLTE design framework using Winter's able-bodied data [47], and its stiffness was used to normalize the stiffness of the other nine feet. Normalizing the range of stiffnesses by the stiffness of the LLTE-optimal foot generated a prosthetic foot stiffness range relative to the LLTE-optimal foot of 75 to 155%.
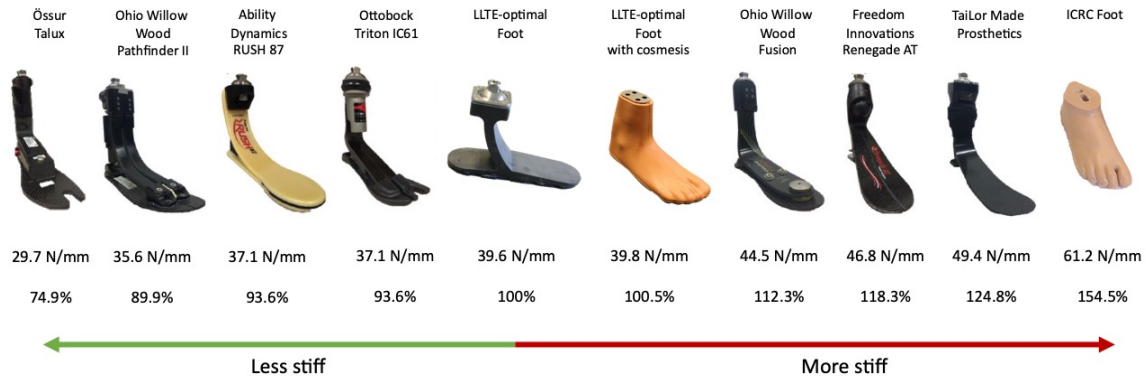
Figure 2-1: Instantaneous stiffness values of several commercially available prosthetic feet sourced for the same hypothetical subject and how they compare to the LLTE-optimal foot stiffness. The load-displacement curves, from which the instantaneous stiffnesses were calculated, were measured according to the ISO 10328 "Static Proof Test for Ankle-Foot Units" and AOPA "Dynamic Keel Test" protocols. The range of stiffness values were used to generate the virtual library of prosthetic foot FEA models, which was used to determine the PFTD functional requirements [46].

While these data provide insight into the range of loads that the PFTD must be able to apply and the range of stiffnesses in commercially available prosthetic feet, they do not provide direct insight into the deflection behavior of prosthetic feet, and therefore, the range of motions the PFTD must enable. To translate the ranges of GRFs and stiffnesses into ranges of foot deflections, a virtual library of prosthetic foot FEA models was created to characterize the behavior of the full range of commercially available prosthetic feet under loading. The foot designs in the virtual foot library were based on a parametric single-keel foot architecture with known constitutive behavior that had been developed in previous works [26, 35]. With this architecture, the overall foot stiffness can be adjusted by varying the thickness of the foot structure. This allows a single foot architecture to represent the full range of commercially available prostheses, whose stiffnesses vary between and within weight categories (Tables 2.2-2.3). The virtual foot library was developed from approximately 200 previously designed feet that had been optimized for a variety of user characteristics through the LLTE design framework. As shown in Table 2.2, the foot model stiffnesses were scaled linearly with the subject mass to create subject mass categories. Within each

Table 2.2: A sample prosthetic foot model scaled for three subject mass categories. Since the GRFs and foot stiffness scale linearly with the subject mass, the LLTE value remains approximately constant.

Foot model			
Subject mass (kg)	40	100	166
GRF_x range (N)	[-80.5, 77.2]	[-201, 193]	[-334, 320]
GRF_y range (N)	[215, 428]	[537, 1071]	[891, 1778]
Relative stiffness (-)	100%		
LLTE (-)	0.111	0.115	0.116

subject mass category, the foot model stiffnesses were further scaled by the range of prosthetic foot stiffnesses that were derived from Webber and Kaufman's comparative study, as previously discussed (Table 2.3). To capture the full range of prosthetic feet and still maintain a reasonable computational effort, we used seven subject mass categories (40, 60, 70, 100, 166, and 200 kg) and three stiffness subcategories (75%, 100%, and 155%), resulting in 18 groups (one group would be 70kg subject mass with 155% stiffness, for example) and approximately 4,000 foot designs. This virtual foot library contains constitutive FEA models of prosthetic feet that represent the full range of commercially available feet and can therefore be used to determine the mechanical behavior of any prosthetic foot that might be tested on the PFTD.

We used this virtual foot library to determine the ranges of foot deflections that could be expected from the full commercial range of prosthetic feet (Table 2.1). This ultimately determined the PFTD's ranges of motion (Table 3.1), which is discussed later in Section 3.1. To do so, we applied the ranges of GRFs to all the FEA foot models in the virtual foot library and measured the deflection behavior, in terms of the LLTE kinematic variables. More specifically, we applied the full GRF ranges for each subject mass to the FEA model of each prosthetic foot that could experience those loads and recorded the deflections. The range for each variable, shown in Table

Table 2.3: A sample prosthetic foot model in the 100kg subject mass category scaled for three stiffness categories. Since the GRFs do not scale linearly with the foot stiffness, the LLTE value changes, increasing as the relative stiffness deviates from the LLTE-optimal stiffness of 100%.

Foot model			
Subject mass (kg)	100		
GRF_x range (N)	[-201, 193]		
GRF_y range (N)	[537, 1071]		
Relative stiffness (-)	75%	100%	155%
LLTE (-)	0.122	0.115	0.198

2.1, was determined from the maximum and minimum of all possible deflections.

2.2 LLTE Accuracy

The second critical functional requirement is the required LLTE accuracy, which was chosen to be similar to the resolution of an average adult human's perception. Shepherd et al. [41] measured the Just Noticeable Difference in ankle stiffness, which represents the smallest percent change in stiffness that can reliably be identified by a subject as an increase or decrease in stiffness, to range from 3.7 to 13.6%, with a mean of 7.7 ± 1.3%. The PFTD was designed to have a similar level of perception, or more specifically, to be able to distinguish between two feet that varied in stiffness by 7.7%. To accomplish this, the PFTD must be able to measure an LLTE value with an accuracy that corresponds to half of the minimum change in stiffness, or 3.85%. The required accuracy corresponds to half of 7.7% rather than the full value to ensure that two feet that vary in stiffness by 7.7% will produce distinct LLTE values. In other words, the error bars for each measured LLTE value must not overlap, so the total difference in stiffness (7.7%) is divided by two to result in a maximum error in each value of 3.85%.

To translate the minimum change in stiffness of a foot that the PFTD must be able to detect into a required LLTE accuracy, effectively the maximum allowable error in LLTE, the previously-described virtual library of prosthetic foot FEA models was used to characterize the relationship between stiffness and LLTE. We found that a change in prosthetic foot stiffness of 3.85% correlated on average with a change in LLTE of 0.0059. To do this, we first measured the LLTE value of each of the original foot models. Then, we changed the stiffness of the foot models by 3.85% and measured the LLTE values of the modified foot models. By comparing the LLTE values of the original and modified feet, we were able to calculate the change in LLTE value that corresponded to a 3.85% change in stiffness. To measure a change in stiffness of 3.85%, thereby distinguishing between two prosthetic feet that varied in stiffness by 7.7%, we would need to be able to measure the LLTE values with an error less than 0.0059 (Table 2.1).

Chapter 3

Kinetics, Kinematics, and Error Analysis

The PFTD was designed to apply loads in the ankle reference frame to simplify the device architecture. As shown in Fig. 3-1, it is composed of three subsystems: the vertical stage module, which applies a vertical force and measures vertical displacement; the horizontal stage module, which applies a horizontal force and measures horizontal displacement; and the rocker platform, which applies an angled force and measures angular displacement. The rocker platform represents the ground and works in concert with the vertical and horizontal stage modules to independently apply GRFs at specific CoP locations. This architecture with three degrees of actuation was chosen so that the PFTD could apply specific and independent GRFs to a foot at a specific CoP. This allows us to apply walking loads to a foot, measure the deformation, and calculate the foot's LLTE value. The layout presented in Fig. 3-1 resulted from the following analysis but has been included here to give the reader a clear picture of function. More details about the architecture design, including design trade-offs and error management, will be discussed in Section 4.

a.

A, Q – BLDC servo motor
B, P – Linear stage
C, K, O – Load cell
D, N – Flexure mechanism
E – Pylon
F – Prosthetic foot
G – Rocker platform
H – Shaft/bearings
I – Rotary encoder
J – Spherical joint
L – Linear actuator
M – Universal joint

b.
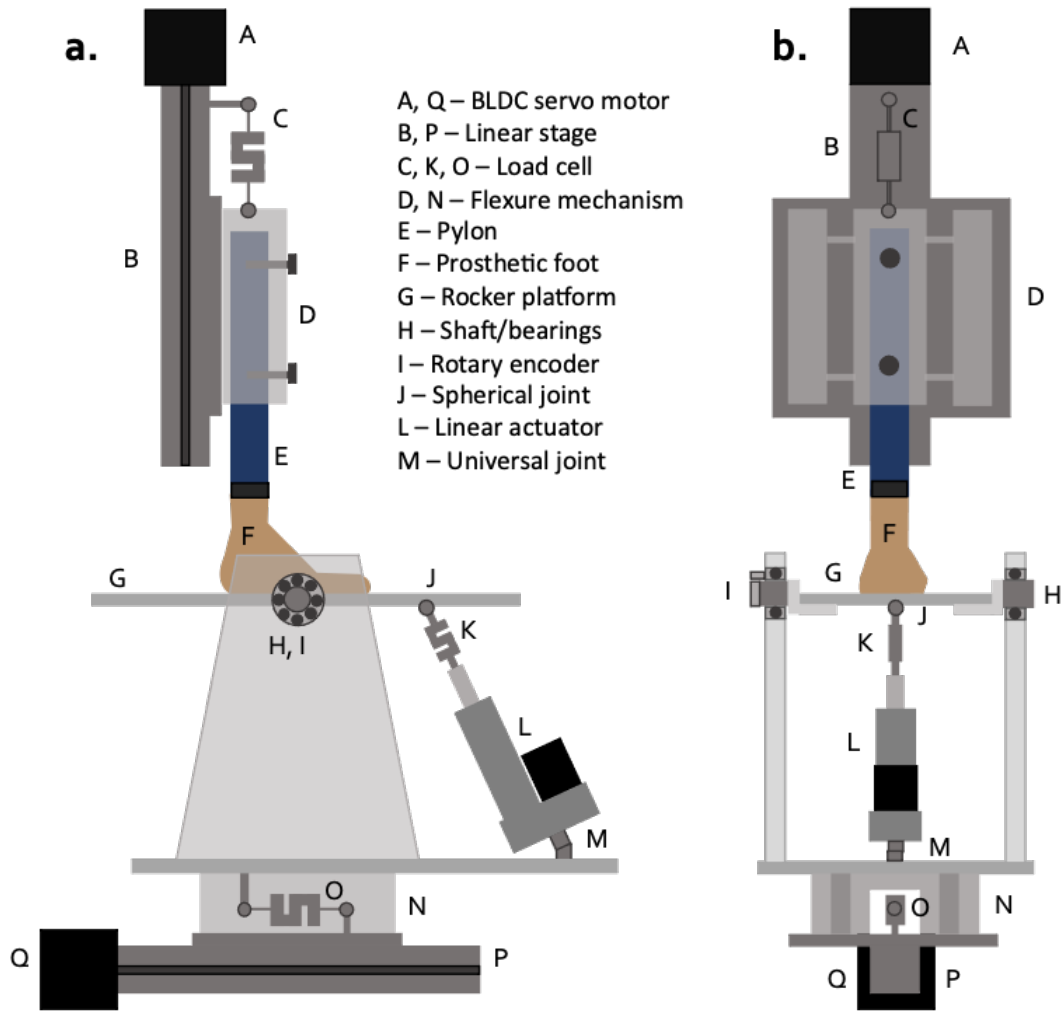
Figure 3-1: Side view (a) and front view (b) schematics of the PFTD and prosthetic foot with components and structural elements labeled. The PFTD consists of a vertical stage module (A-D), horizontal stage module (N-Q), and rocker platform (G-M).

To design and control the PFTD to be able to measure LLTE, we must understand the relationships between the variables that are part of the LLTE calculation and those controlled or measured by the PFTD. These will be referred to as the LLTE variables (GRF_x, GRF_y, CoP, x_knee, y_knee, $\theta_\text{lower leg}$) and PFTD variables ($F_\text{stage,x}$, $F_\text{stage,y}$, F_rocker, Δx_stage, Δy_stage, θ_rocker), respectively, as displayed in Fig. 3-2. Figure 3-2 contains a schematic that illustrates the forces, displacements, and constants relevant to the PFTD, displayed in the ankle reference frame, in which the knee is stationary; in contrast, the schematic in Fig. 1-1 is displayed in the global reference frame, in which the ground is stationary. In Fig. 3-2, the LLTE kinetic and kinematic variables are shown in purple, the PFTD kinetic variables are shown in blue, the PFTD kinematic variables are shown in red, and various constant or dependent variables are shown in black. The system of equations that relates the LLTE variables to the PFTD variables, derived from trigonometry, are as follows:

$$x_\text{knee} = (l_\text{shank} + y_0 + \Delta y_\text{stage}) \sin \Theta_\text{rocker} + x_0(1 - \cos \Theta_\text{rocker}) \tag{3.1}$$

$$-\Delta x_\text{stage} \cos \Theta_\text{rocker} \tag{3.2}$$

$$y_\text{knee} = (l_\text{shank} + y_0 + \Delta y_\text{stage}) \cos \Theta_\text{rocker} + (x_0 + \Delta x_\text{stage}) \sin \Theta_\text{rocker} \tag{3.3}$$

$$\Theta_\text{lower leg} = \Theta_\text{rocker} \tag{3.4}$$

$$GRF_\text{x} = F_\text{stage,y} \sin \Theta_\text{rocker} + F_\text{stage,x} \cos \Theta_\text{rocker} \tag{3.5}$$

$$GRF_\text{y} = F_\text{stage,y} \cos \Theta_\text{rocker} + F_\text{stage,x} \sin \Theta_\text{rocker} \tag{3.6}$$

$$CoP = \frac{F_\text{rocker} d_\text{la} \cos \Theta_\text{la}}{F_\text{stage,y} \cos \Theta_\text{rocker} - F_\text{stage,x} \sin \Theta_\text{rocker}} + x_0 \tag{3.7}$$

In Eqns. 3.1-3.7, l_shank represents the shank length; y_0 represents the height of the unloaded foot; x_0 represents the distance between the ankle center of the unloaded foot and the rocker platform axis of rotation; Δx_stage, Δy_stage, and θ_rocker represent the displacements of the horizontal stage, vertical stage, and rocker platform, respectively; $F_\text{stage,x}$, $F_\text{stage,y}$, and F_rocker represent the forces applied by the horizontal stage, vertical stage, and rocker platform, respectively, d_la represents the distance between the rocker
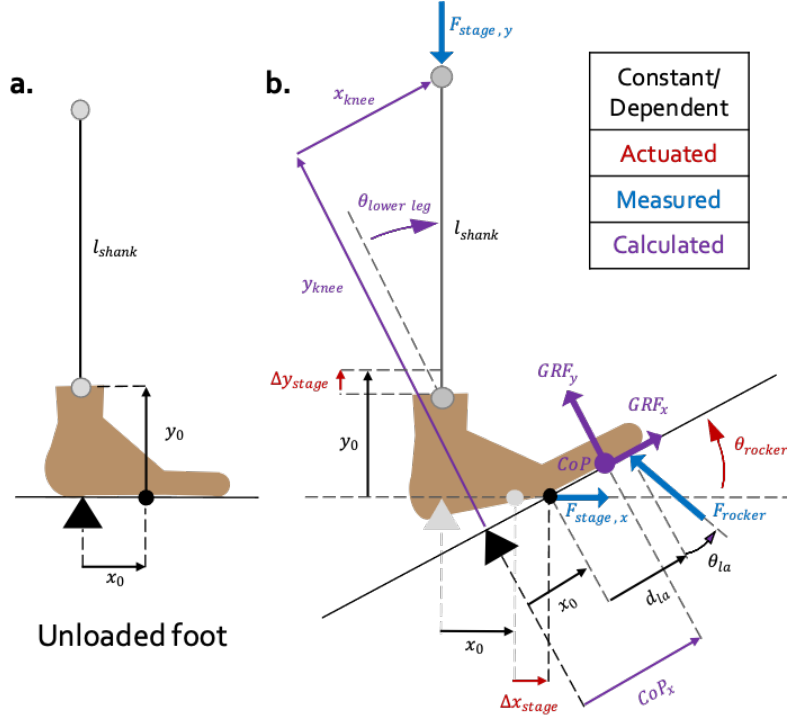
Figure 3-2: Schematic of the loads applied by the PFTD to a prosthetic foot during testing (PFTD kinetic variables: $F_{\text{stage,x}}$, $F_{\text{stage,y}}$, and F_{rocker}, in blue), the actuated variables of the PFTD (PFTD kinematic variables: Δx_{stage}, Δy_{stage}, and θ_{rocker}, in red), the reference loads applied to the foot (LLTE kinetic variables: GRF_{x}, GRF_{y}, CoP, in purple), and the calculated knee location and shank orientation (LLTE kinematic variables: x_{knee}, y_{knee}, and $\Theta_{\text{lower leg}}$, in purple). a) Unloaded foot. b) Loaded foot.

platform axis of rotation and the point at which F_{rocker} is applied; and Θ_{la} represents the angle of F_{rocker} relative to the rocker platform's normal vector.

3.1 Calculating PFTD Variable Ranges

To translate the ranges of reference loads and prosthetic foot deflections (high-level functional requirements derived in Section 2.1) to ranges of PFTD loads and motions (low-level functional requirements), we performed uncertainty analysis using the virtual prosthetic foot FEA model library described in Section 2.1. For each group in the library (one group would be 70 kg subject mass with 155% stiffness, for example), GRFs from Winter's able-bodied level ground walking data [47], scaled by the subject mass, were applied to the feet, and the knee locations and shank orientations

were calculated using the constitutive models. These LLTE kinematic values were transformed into PFTD kinematic variables using the system of equations in Section 3 (Eqns. 3.1-3.7). Next, the LLTE kinetic variables and PFTD kinematic variables were used to calculate the PFTD kinetic variables, using the same system of equations. This provided the full range of PFTD variables that would be required to apply the reference loads to the full range of commercially available feet (Table 3.1).

3.2   Calculating PFTD Variable Error Sensitivities

To design the structure and choose the components of the PFTD to satisfy the LLTE accuracy requirement (Table 2.1), a parameter study was performed to determine how sensitive the LLTE value is to errors in each of the PFTD variables. We refer to these sensitivities as the error sensitivities of the PFTD variables. In the parameter study, error was introduced to one PFTD variable at a time to determine the effect of the variable change on the LLTE value. By calculating the error sensitivity of each variable, we could predict the error in LLTE caused by the errors in each PFTD variable (which may be due to component nonrepeatability, structural stiffness, or machining tolerances, for example) and thus design the PFTD to have an acceptable maximum error.

Figure 3-3 illustrates the parameter study methodology implemented for one of the PFTD variables, F_{rocker}. For each group in the virtual foot model library, error (as either a percent error or absolute error) was introduced to each variable, and the average change in LLTE was calculated (Fig. 3-3a). For each PFTD variable, this resulted in 18 error sensitivity values, the maximum of which was chosen as the overall error sensitivity (Fig. 3-3b). The absolute and percent error sensitivity values for all PFTD variables, subject masses, and foot stiffnesses are included in Appendix A. To make the error sensitivity values more intuitive, the error sensitivities of each variable were translated into required accuracies by dividing the required LLTE accuracy, 0.0059, by the error sensitivities. These required accuracies are displayed in Table 3.2 and represent the maximum allowable error in each variable if 100% of

35

Table 3.1: The low-level functional requirements of the PFTD, derived from the high-level functional requirements (Table 2.1) and the system of equations that relates the LLTE variables to the PFTD variables (Eqns. 3.1-3.7). The ranges of the PFTD variables shown here would enable the PFTD to apply the reference loads to the full range of commercially available feet.

Category	Requirement	Definition	Range [min, max]
PFTD Kinetic Variable Ranges	Range of $F_{\text{stage,x}}$	The range of forces the horizontal stage module must be able to apply and measure	[-1002 N, 337.2 N]
	Range of $F_{\text{stage,y}}$	The range of forces the vertical stage module must be able to apply and measure	[211.1 N, 2160 N]
	Range of F_{rocker}	The range of forces the rocker platform must be able to apply and measure	[-1767 N, 2013 N]
PFTD Kinematic Variable Ranges	Range of Θ_{rocker}	The range of positions the rocker platform must be able to provide and measure	[-21.6 deg, 39.3 deg]
	Range of Δx_{stage}	The range of positions the horizontal stage module must be able to provide and measure	[-1.59 cm, 5.53 cm]
	Range of Δy_{stage}	The range of positions the vertical stage module must be able to provide and measure	[-5.04 cm, 3.50 cm]
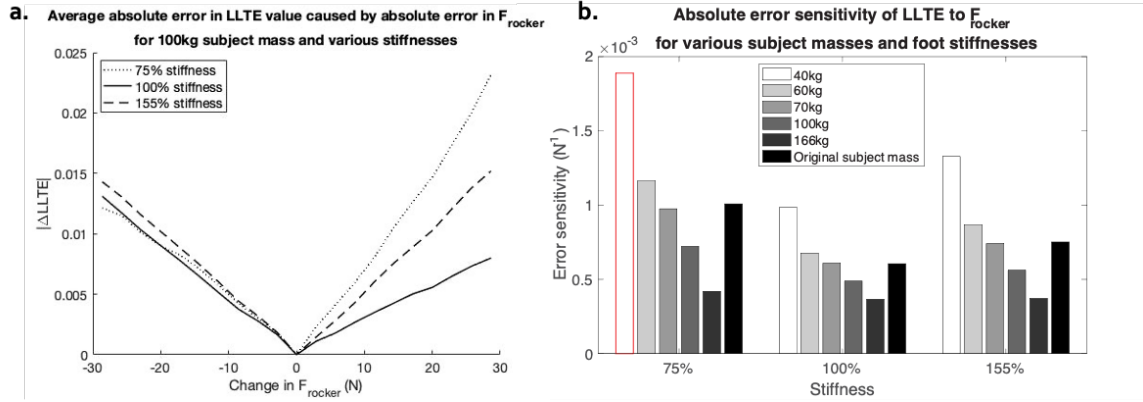
Figure 3-3: PFTD variable error sensitivity parameter study methodology, shown for the absolute error sensitivity of one variable, F_{rocker}. a) Average absolute error in LLTE value caused by absolute error in F_{rocker} for the 100 kg subject mass category and various stiffness categories. The absolute error sensitivity of LLTE to F_{rocker} for each stiffness is calculated as the slope of each best fit line. b) Absolute error sensitivity of LLTE to F_{rocker} for various subject mass and foot stiffness categories. These values are equal to the slope of the lines in a). The maximum of these values (outlined in red) is used as the absolute error sensitivity value. In the case of F_{rocker}, the 40 kg subject mass and 75% stiffness group resulted in the maximum error sensitivity of 0.0019 N^{-1}. This means that an error of 1 N in F_{rocker} causes an error of 0.0019 in the LLTE value. The same process is used to find the absolute and percent error sensitivities of each PFTD variable, which are then converted into required accuracies (Table 3.2).

the PFTD error were due to that variable. From these values, it is clear that errors in Θ_{rocker}, F_{rocker}, and $F_{\text{stage,y}}$ were predicted to have the greatest influence on the output LLTE error.

Table 3.2: The required accuracy of each PFTD variable, which represents the maximum error each variable could have if 100% of the allowable PFTD error was allotted to a single variable. Required accuracies are displayed as both absolute and percent error values.

PFTD Variable Required Accuracies		
Variable	Absolute	Percent
$F_{\text{stage,x}}$	± 9.14 N	$\pm 4.45\%$
$F_{\text{stage,y}}$	± 6.70 N	$\pm 1.32\%$
F_{rocker}	± 3.19 N	$\pm 1.20\%$
θ_{rocker}	± 0.288 deg	$\pm 1.87\%$
Δx_{stage}	± 4.96 mm	$\pm 33.2\%$
Δy_{stage}	± 2.50 cm	$\pm 123\%$

We conducted this parameter study to represent the range of prosthetic feet that will be tested on the PFTD, using most of the full virtual foot model library but excluding the 200 kg subject mass category. This was done because including the 200 kg category resulted in significantly higher error sensitivities, and out of the 62 commercially available feet that were compiled from catalogs, only one was designed to accommodate a 200 kg user, and the subsequent highest subject mass was 166 kg [2, 8, 15, 29, 30]. There were two portions of the parameter study: one calculated the absolute error sensitivities, or the sensitivity of the output LLTE value to absolute error in the variables, and the other calculated the percent error sensitivities, or the sensitivity of the output LLTE value to percent error in the variables. The purpose of this was to be able to predict the effect of error in the PFTD components, which can be reported as either absolute error or percent error.

3.3 Calculating LLTE Kinetic Variable Error Sensitivities

To design the control scheme of the PFTD to satisfy the LLTE accuracy requirement (Table 2.1), a second parameter study was performed to determine how sensitive the

LLTE value is to errors in each of the LLTE kinetic variables. We refer to these sensitivities as the error sensitivities of the LLTE kinetic variables. In the parameter study, error was introduced to one LLTE kinetic variable at a time to determine the effect of the variable change on the LLTE value. This allowed us to predict the error in LLTE caused by the errors in each LLTE kinetic variable, which may arise due to limitations in the PFTD resolution or control scheme. Using the error sensitivity for each variable, we can design the PFTD control scheme to have an acceptable maximum error. This error is separate from the LLTE error caused by errors in each PFTD variable, which are related to the structural design and components, as discussed in Section 3.2.

Since the PFTD does not directly control the LLTE kinetic variables, and each foot deforms differently under loading, the system of equations that relates the LLTE variables to the PFTD variables (Eqns. 3.1-3.7) is unsolvable, and therefore, the control scheme must be iterative. The PFTD adjusts its kinematic variables until the LLTE kinetic variables come within an error threshold of the reference load values. The errors between the LLTE kinetic variable values achieved by the PFTD and those in the reference data result in an error in the output LLTE value. Thresholds for these errors must be chosen so that the PFTD satisfies its accuracy requirement without overly restricting the control scheme such that it is difficult to converge on the target loading case. These thresholds are determined from the error sensitivities of the LLTE kinetic variables.

This parameter study utilized the same methodology as the first parameter study, described in Section 3.2 and illustrated in Fig. 3-3. However, in this second parameter study, the error introduced into the CoP variable was absolute and the error introduced into the GRF variables was a percentage of the range of GRF values. The latter means that the GRF thresholds will be larger when testing a foot in the 100 kg category than when testing a foot in the 70 kg category. By using a percentage instead of an absolute error value, we ensure the threshold is not overly conservative during testing. We are able to do this because each time a new foot is tested, we can change the threshold values to correspond to the subject mass of the user. This

is unlike the component errors modeled in the parameter study previously discussed in Section 3.2, which are constant no matter which foot is being tested. We use a percentage of the range instead of a percentage of the value so that the threshold is not overly conservative for small GRF values or overly loose for large GRF values throughout stance.

To make the error sensitivity values more intuitive, the error sensitivities of each variable were translated into required accuracies by dividing the required LLTE accuracy by the error sensitivities. These required accuracies are displayed in Table 3.3 and represent the maximum allowable error in each variable if 100% of the PFTD error were due to error in that variable. In reality, the thresholds of the variables will be determined by the difference between the total allowable PFTD error and the permanent error introduced by electrical and structural components. The thresholds can be dynamically updated as the PFTD operates, since the LLTE kinetic variables share a total error budget. For example, the error threshold for GRF_y can be relatively larger if the GRF_x achieved by the PFTD is very close to the GRF_x target reference value, than if the GRF_x achieved by the PFTD is very far from the GRF_x target reference value.

Table 3.3: The required accuracy of each LLTE kinetic variable, which represents the maximum error each variable could have if 100% of the allowable PFTD error was allotted to a single variable. GRF required accuracies are displayed as a percentage of the range and the CoP required accuracy is displayed as absolute error.

LLTE Kinetic Variable Required Accuracies	
Variable	Required Accuracy
GRF_x	±10.8% of range
GRF_y	±2.58% of range
CoP	±1.21 mm

The PFTD variables ranges (Table 3.1) and error sensitivities (Table 3.2) as well as the LLTE kinetic variable error sensitivities (Table 3.3) proved instrumental in the machine design process. They established requirements that informed PFTD

dimensions, components, and structural elements.

Chapter 4

Machine Design

The PFTD architecture is divided into three subsystems, each of which have a degree of actuation and measurement: the vertical stage module, horizontal stage module, and rocker platform (Fig. 4-1). In the vertical stage module, an AC brushless servo motor actuates a linear stage, which is connected to the pylon and prosthetic foot via a load cell, which is constrained by a flexure mechanism. The flexure mechanism, a parallel translator that utilizes blade flexures [7], was designed to be highly compliant in the direction of the load cell measurement (vertical motion) and highly resistant to any moments or horizontal loads. More details about the flexure mechanism design are included in Section 4.3. In the horizontal stage module, an AC brushless servo motor actuates a linear stage, which is connected to the rocker platform via a load cell, which is constrained by a similar flexure mechanism. The vertical and horizontal displacements are measured by the motor encoders in the vertical and horizontal stage modules, respectively. The rocker platform is attached to the top of the horizontal stage module and consists of a platform that rotates around an axis of rotation and is actuated by a rod-type linear actuator that is powered by an AC brushless servo motor. A load cell in line with the linear actuator measures the force applied to the rocker platform and a rotary encoder is attached to the axis of rotation and measures the angular motion.

Figure 4-1: A rendered CAD image of the PFTD and prosthetic foot.

Specific elements of this architecture were chosen to satisfy the functional requirements discussed in Section 2 in a cost-effective manner that limited the total measurement error. For example, we chose to design and build the vertical stage module instead of using a universal testing machine because the error caused by off-axis loading during toe or heel loading would have exceeded the allowable error in $F_{\text{stage,y}}$. We chose to actuate the rocker platform with a linear actuator beneath the platform rather than with a servo motor in line with the axis of rotation because the linear actuator provides better mechanical advantage and avoids gearbox backlash issues, and the rocker platform does not require the ability to complete multiple rotations. Furthermore, a load cell in line with the linear actuator provides higher accuracy than would a torque sensor in line with the axis of rotation. As a final example, we chose to mount the rocker platform on top of the horizontal stage module, as opposed to vice versa, because it resulted in lower error sensitivity values, and therefore, a higher overall LLTE accuracy.

4.1 Component Selection

The components, including motors, stages, linear actuator, load cells, and rotary encoder, were chosen to provide and withstand the necessary loads and ranges of motion as well as to minimize error. The components, along with their relevant error specifications, are listed in Table 4.1. Table 4.2 lists the significant component errors that affect each PFTD variable. The error specifications of the components were multiplied by the error sensitivity values of the corresponding PFTD variables (derived via the parameter study discussed in Section 3.2) to determine how much each variable and component contributed to the total LLTE error (Table 4.2). Figure 4-2 displays the distribution of the total error budget amongst both the variables and components, with the remaining error budget displayed as white space, and illustrates which specific component errors make up the error in each PFTD variable. The remaining error budget (white space) will be distributed between structural errors, control scheme errors (discussed in Sections 3.3 and 5), and any unmodeled errors.

Table 4.1: Component information, including brand, model number, and relevant error specifications. The components were chosen such that the errors in each variable would be significantly less than the required accuracies displayed in Table 3.2.

Subsystem	Brand	Component	Model/Part #	Relevant error	Error value
Horizontal stage module	PT *Auckland, New Zealand*	Steel S-Type Tension/ Compression Load Cell – 4000	PT4000-500lb	Repeatability	0.2224 N
	Nippon Bearing *Ojiya, Niigata, Japan*	BG Actuator	BG4610B440H/ AZ/Z21028	Repeatability	0.003 mm
				Positioning Accuracy	0.035 mm
	Automation Direct *Cumming, GA, USA*	SureServo medium inertia AC brushless servo motor	SVM-210	Repeatability	1.08 deg
Vertical stage module	PT *Auckland, New Zealand*	Steel S-Type Tension/ Compression Load Cell – 4000	PT4000-1klb	Repeatability	0.4448 N
	Nippon Bearing *Ojiya, Niigata, Japan*	BG Actuator	BG4610B640H/ RZ/Z21060	Repeatability	0.003 mm
				Positioning Accuracy	0.04 mm
	Automation Direct *Cumming, GA, USA*	SureServo medium inertia AC brushless servo motor	SVM-220	Repeatability	1.08 deg
Rocker Platform	PT *Auckland, New Zealand*	Steel S-Type Tension/ Compression Load Cell – 4000	PT4000-1klb	Repeatability	0.4448 N
	Renishaw *Wotton-under-Edge, UK*	Resolute Absolute Encoder System with RESA30	RESA30USA052B RA26BBA052B15F	Accuracy	0.0015 deg
	Thomson *Radford, VA, USA*	T90 Precision Linear Actuator	T09SXXXXB2510-00200XNXX	N/A	N/A
		BGM Parallel Mounting Belt Kit	BGM41-3-CCAK4P09AS+XX	N/A	N/A
	Kollmorgen *Radford, VA, USA*	AKM 2G Servo Motor	AKM2G-42E-ANDNCA00	N/A	N/A
All	National Instruments *Austin, TX, USA*	CompactRio	cRIO-9042	N/A	N/A
		C Series Universal Analog Input Module	NI-9219, 785994-01	Gain error	0.2%

Table 4.2: Component error breakdown. The components were chosen such that the errors in each variable would be significantly less than the required accuracies displayed in Table 3.2.

PFTD Variable	Relevant component error	Error type	Error sensitivity	Error value	Induced LLTE error (-)	Share of total allowable error
$F_{\text{stage,x}}$	Horizontal load cell repeatability	Absolute	6.5e-4 -/N	0.22 N	1.4e-4	2.4%
	Horizontal load cell amplifier gain error	Percent	0.0013 -/%	0.2%	2.7e-4	4.5%
$F_{\text{stage,y}}$	Vertical load cell repeatability	Absolute	8.8e-4 -/N	0.44 N	3.9e-4	6.6%
	Vertical load cell amplifier gain error	Percent	0.0045 -/%	0.2%	0.9e-4	15.2%
F_{rocker}	Rocker load cell repeatability	Absolute	0.0019 -/N	0.44 N	8.2e-4	13.8%
	Rocker load cell amplifier gain error	Percent	0.0049 -/%	0.2%	9.9e-4	16.7%
Θ_{rocker}	Rotary encoder accuracy	Absolute	0.021 -/deg	0.0015 deg	3.1e-5	0.5%
Δx_{stage}	Horizontal motor repeatability	Absolute	0.0012 -/mm	0.03 mm	3.6e-5	0.6%
	Horizontal stage repeatability and accuracy			0.038 mm	4.5e-5	0.8%
Δy_{stage}	Vertical motor repeatability	Absolute	0.0024 -/mm	0.031 mm	7.3e-6	0.1%
	Vertical stage repeatability and accuracy			0.043 mm	1.0e-5	0.2%
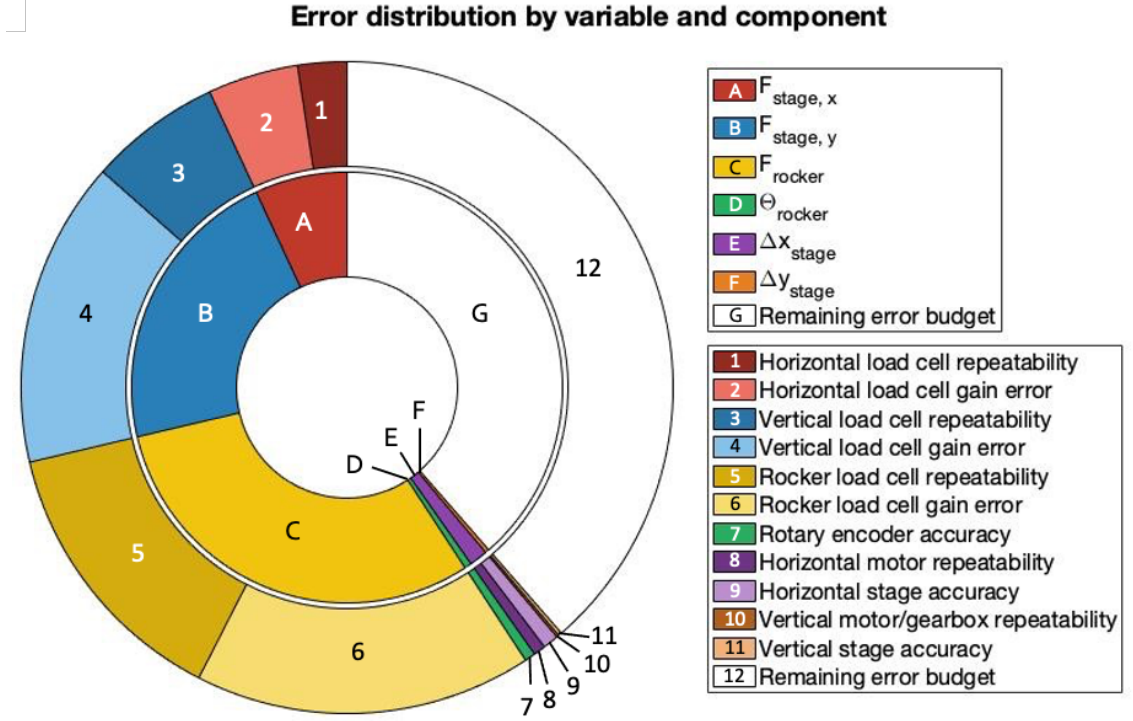
Figure 4-2: The distribution of total allowable PFTD error organized by PFTD variable and component (Table 4.2). These values are a function of PFTD variable error sensitivities and component error specifications. The remaining error budget is shown in white. The most significant sources of error are $F_{\text{stage,x}}$, $F_{\text{stage,y}}$, and F_{rocker}.

4.2 x_0 Optimization

The distance between the unloaded ankle center and the rocker platform axis along the platform, a constant referred to as x_0, was optimized to minimize the actuator loading and error sensitivities. x_0 is present in the system of equations relating the LLTE variables to the PFTD variables (Eqns. 3.1-3.7) and therefore impacts the ranges and error sensitivities of the PFTD variables. To find the x_0 value that minimized total PFTD error, the previously discussed parameter studies used to determine the PFTD variable ranges and error sensitivities (Sections 3.1-3.2) were conducted multiple times with different values of x_0. Figure 4-3 illustrates how the error sensitivities of the PFTD variables vary with x_0. To minimize the error sensitivities of the most relevant variables, the variable ranges, and the total LLTE error, we set $x_0 = 0.085$ m, which corresponds to the rocker platform axis of rotation being located at the midpoint
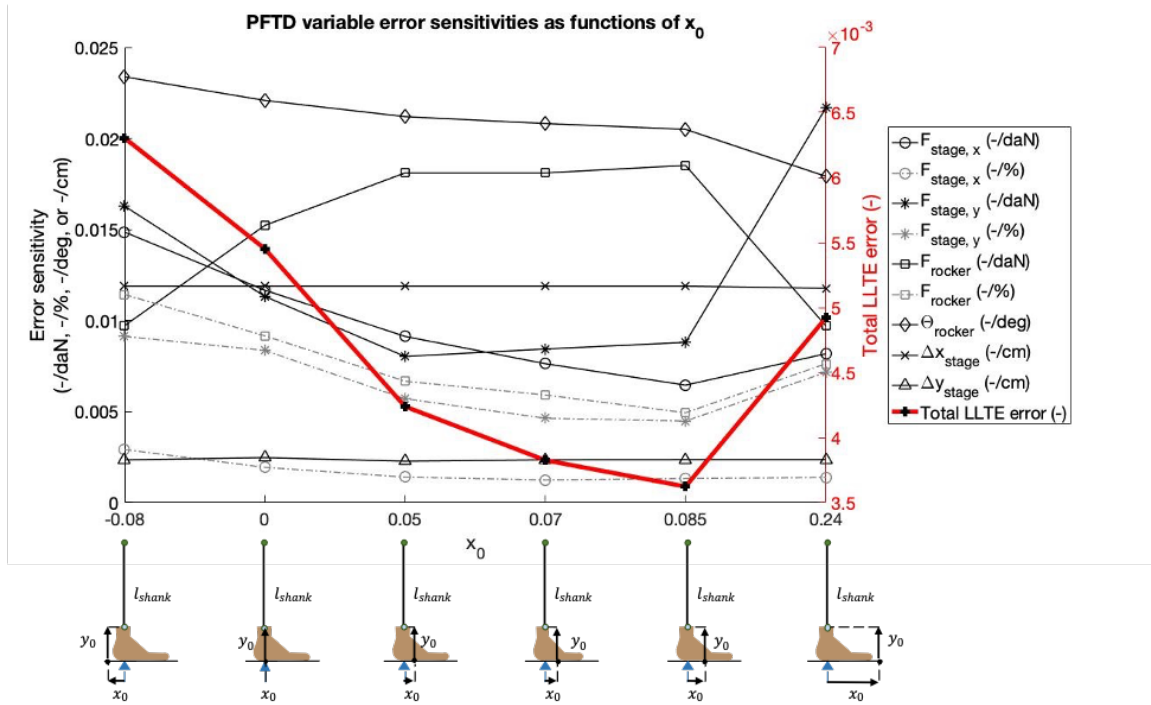
Figure 4-3: The relevant PFTD variable error sensitivities and total LLTE error as they vary with x_0. The physical meaning of each x_0 value is displayed using foot models underneath the plot. To minimize the total LLTE error, x_0 was set to 0.085, which corresponds to the rocker platform axis of rotation being located at the midpoint of the longest commercially available foot.

of the longest commercially available foot. This makes intuitive sense, since with the axis of rotation at the midpoint of a foot, the loads are approximately evenly distributed on either side and the maximum moment arm is minimized.

4.3   Flexure Mechanism Design

The parallel translator flexure mechanisms (Fig. 4-4) were designed to be highly compliant in the direction of the load cell measurement (x-direction) and highly resistant to any loads in the y-direction or moments around the z-axis. This ensured that the flexure mechanism introduced minimal error into the load cell reading while constraining the load cell such that it experienced minimal off-axis loading. Using a MATLAB script that implemented beam-bending equations [38] to analytically com-
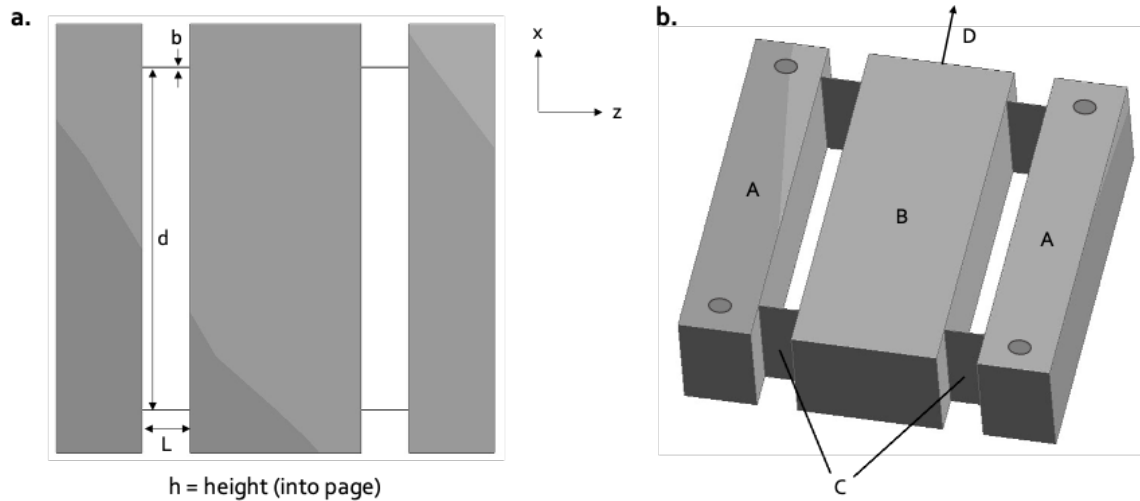
Figure 4-4: Parallel translator flexure mechanism architecture designed to constrain the horizontal and vertical load cells, optimized to minimize stiffness in the x-direction while satisfying constraints on stress safety factor as well as stiffness in the y-direction and around the z-axis. a) Top view with coordinate system and parameterized dimensions labeled: b, L, and h represent the width, length, and height of the blade flexures and d represents the distance between the blade flexures. b) Isometric view with components labeled: rigid bodies A are grounded, rigid body B translates in the D-direction, and blade flexures C allow the degree of freedom.

pute the stiffness in the x-direction, k_x, and the minimum stress safety factor, we built an optimization scheme to minimize k_x while satisfying stress safety factor and dimensional constraints. This model was validated using commercial FEA software (Ansys, 2020R1 Student Edition). The optimal parameter values are displayed in Table 4.3 and the resulting stiffness and stress safety factor values are displayed in Table 4.4.

Table 4.3: Parameter values of the flexure mechanisms in the horizontal and vertical stage modules.

Parameter	Horizontal stage module Value	Vertical stage module Value
L	15 cm	15 cm
b	2.3 mm	1.1 mm
h	15 cm	15 cm
d	40 cm	40 cm

Table 4.4: Stiffness and stress safety factor values of the flexure mechanisms in the horizontal and vertical stage modules. The flexure mechanisms were optimized to minimize k_x, the stiffness in the x-direction (Fig. 11), while satisfying constraints on stiffness in the y-direction and stress safety factor.

Property	Horizontal stage module Value	Vertical stage module Value
k_x	1.54e5 N/m	1.68e4 N/m
Load cell to mechanism stiffness ratio	51.7	946
Safety factor	10	10

Chapter 5

Conclusions and Future Work

The aim of this work was to design a novel mechatronic prosthetic foot testing device capable of applying specific and uncoupled GRFs to any CoP on a foot and measuring its deflection, through which the device could measure the LLTE value and thus predict the walking performance of any passive prosthetic foot.

Using previous studies and commercial prosthetic foot catalogs, we determined the high-level functional requirements of the PFTD such that it would be able to meaningfully measure the full commercial range of prosthetic feet. This required quantifying the ranges of reference loads and prosthetic foot deflections as well as the required accuracy for measuring the LLTE. We created a virtual library of prosthetic foot FEA models that represented the full range of commercially available feet and could therefore be used to determine the mechanical behavior of any prosthetic foot that might be tested on the PFTD. We derived the system of equations relating the variables used to calculate the LLTE value and those used to control the PFTD. We conducted parameter studies, which employed this system of equations and the virtual foot library, to understand the ranges of PFTD variables as well as how error in each of the PFTD variables yielded error in the measured LLTE value. We used this understanding to design an architecture and select components that were predicted to allow the PFTD to satisfy a set of functional requirements and meaningfully measure the LLTE value of any passive prosthetic foot. We conducted an additional parameter study using the virtual foot library to determine how error in each of the LLTE

kinetic variables created error in the LLTE value, which will be critical to designing a successful control scheme and achieving the required LLTE accuracy. In this work, we identified the requirements for a testing device that could measure the LLTE value of any passive prosthetic foot, which has the potential to unlock the value of the LLTE metric for the prosthetics community.

Unlike existing testing devices that have been designed to measure specific mechanical properties, the PFTD was designed to directly predict the walking performance of a prosthetic foot by measuring its LLTE value, a universal performance metric that provides a quantitative connection between the mechanical characteristics of a foot and the expected gait of an amputee. Furthermore, while most existing devices are limited to one or two degrees of actuation, the PFTD has three degrees of actuation, which allows it to apply uncoupled horizontal and vertical GRFs at a specific CoP and evaluate the response of the foot. Due to this ability, the PFTD is uniquely capable of examining the mechanical behavior of prosthetic feet under specific walking loads.

Throughout this work, we grew to appreciate the level of precision required to design a device that could meaningfully measure the LLTE value of a foot. The LLTE accuracy that correlated to the required measurable change in stiffness was surprisingly strict. Furthermore, the LLTE metric proved to have an unexpectedly high sensitivity to error in the PFTD variables. See Appendix B for the original inherited device design, whose accuracy was designed according to intuition rather than error analysis and therefore did not satisfy the LLTE accuracy requirement discussed in this thesis. The accuracy requirement for the PFTD led to the need for elements of precision engineering, including flexure design and sensitivity analysis, as well as high-precision components. The analyses discussed in this thesis, including the definition of functional requirements, uncertainty analysis, and error sensitivity analyses, help ensure that the device results will be meaningful.

Future work should consist of finalizing the structural design of the PFTD, building the device, designing a control scheme, and validating the device through testing. Performing structural analysis that utilizes homogeneous transformation matrices will

help determine the required stiffness and machining tolerances of several structural elements, such as the external frame and rocker platform foot plate, and ensure that the overall stiffness of the device allows for the satisfaction of the required LLTE accuracy. If it proves infeasible to achieve the stiffness necessary to satisfy the LLTE accuracy requirement, the total allowable error may be increased by restricting the PFTD subject mass range from 40-166 kg to 60-166 kg. Alternatively, the error introduced by the load cell amplifiers may be reduced by designing custom amplifiers instead of using the National Instruments C Series Universal Analog Input Module listed in Table 4.1. While most of the PFTD components have been selected and purchased, the selection of the rocker platform bearings and joints must be finalized, and all applicable components must be calibrated to minimize error. Once the PFTD structure is confirmed, the flexure mechanisms must be optimized to fit within the prescribed dimensions, manufactured via wire EDM, and assembled with the corresponding load cells. The flexure mechanism and load cell systems must then be rigorously characterized and their load-displacement curves documented for use in the control scheme.

Once the PFTD and its control panel is constructed and calibrated, a control scheme must be designed to have two operation modes: manual and automatic. The manual control mode will allow a user to move each actuator independently and read out both the data from each sensor and the calculated LLTE kinetic variables, which will enable the user to manually test a prosthetic foot. The automatic control mode will conduct all the testing required to measure the LLTE value of a prosthetic foot, which will involve loading the foot in several different loading cases that correspond to different moments during the stance phase of walking. As discussed briefly in Section 3.3, for each loading case, the control scheme must iteratively achieve the correct LLTE kinetic variable values to within predetermined error thresholds, which are determined by the variable error sensitivities. The CoP error sensitivity (Table 3.3) is constant, but the GRF error sensitivities are dependent on the subject mass for which the prosthetic foot is designed, which determines the magnitude of the loads being applied to the foot. During the control sequence, the combined total of the

errors in the LLTE kinetic variables combined with their error sensitivities must not exceed the difference between the total allowable error of the PFTD (equivalent to the LLTE accuracy requirement) and the permanent error caused by the PFTD structure and components. To provide a visual aid, the error introduced by the LLTE kinetic variable thresholds in the control scheme must not exceed the white space in Fig. 4-2. There is a level of flexibility in the error thresholds of the LLTE kinetic variables. Since the variables share a total error budget, the required accuracy of each variable can be dynamically updated as the test runs. For example, the error threshold for GRF_y can be larger if the GRF_x achieved by the PFTD is very close to the GRF_x target reference value, than if the GRF_x achieved by the PFTD is very far from the GRF_x target reference value. This dynamic error allotment should help the PFTD converge on the "correct" loading scenario more quickly.

One potential challenge in operating the PFTD is possible slippage between the prosthetic foot and and rocker platform foot plate. Slippage between these two surfaces would introduce error into the Δx_{stage} and Δy_{stage} variables and invalidate the test results. To reduce the chance of slippage, each prosthetic foot should be aligned and preloaded at the beginning of each loading case according to the "Foot Alignment Set-Up" protocol detailed in the AOPA "Dynamic Keel Test" procedure [3]. Furthermore, the control scheme should track the ratio of GRF_y to GRF_x and ensure that it never exceeds the static coefficient of friction between the prosthetic foot and the foot platform.

Once the PFTD is operating correctly, its loading capacity, range of motion, accuracy, and repeatability must be validated to confirm that it satisfies the functional requirements. The loading capacity and range of motion of the PFTD can be validated somewhat simply by experimentally determining the device limits. However, determining the accuracy and repeatability will require more intensive testing. To experimentally measure the accuracy, the PFTD should be used to measure the LLTE value of a foot with a known LLTE value. This is possible if the foot were designed via the LLTE design framework. To experimentally measure the repeatability, the PFTD should be used to measure the LLTE value of the same foot multiple times.

Once complete and validated, the PFTD could be used to measure the LLTE value of any commercially available passive prosthetic foot, which opens up several avenues for research. For example, we expect to use the PFTD to further verify the LLTE design framework by measuring the LLTE values of feet designed via the framework and comparing the experimental values to those predicted by the design framework. Additionally, we plan to measure the LLTE values of feet for which we don't have accurate constitutive models, such as 3D printed feet, and use the experimental results to improve and validate their constitutive models. Another potential research avenue would be measuring and comparing the LLTE values of various prostheses, including commercially available feet, which could provide insight into the effects of various foot features on gait mechanics without human-subject testing. We hope to use the PFTD to systematically and amputee-independently measure and compare the performance of prosthetic devices, which could ultimately improve the development and prescription processes of prostheses.

Appendix A

PFTD Variable Error Sensitivities

The absolute and percent error sensitivities of the PFTD variables for various subject masses and foot stiffnesses are displayed in Figures A-1 and A-2, respectively.

Figure A-1: Absolute error sensitivity of LLTE to each PFTD variable for various subject mass and foot stiffness categories. The maximums off these values (outlined in red) are used as the absolute error sensitivities.
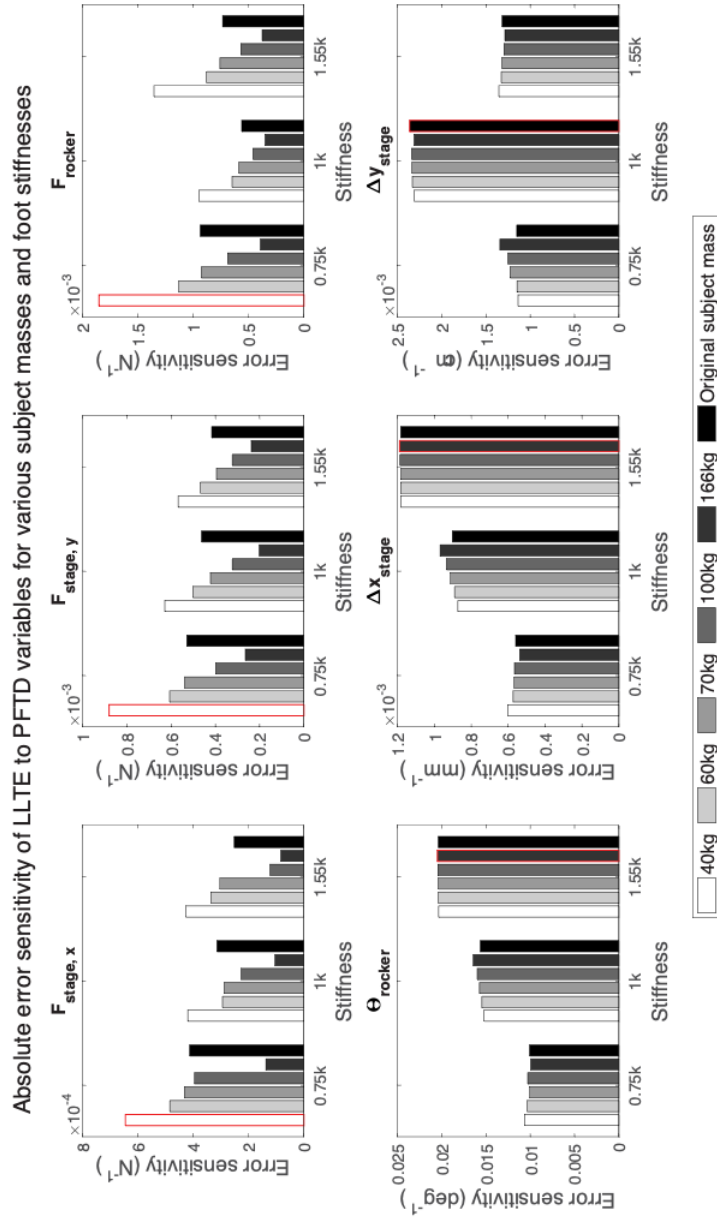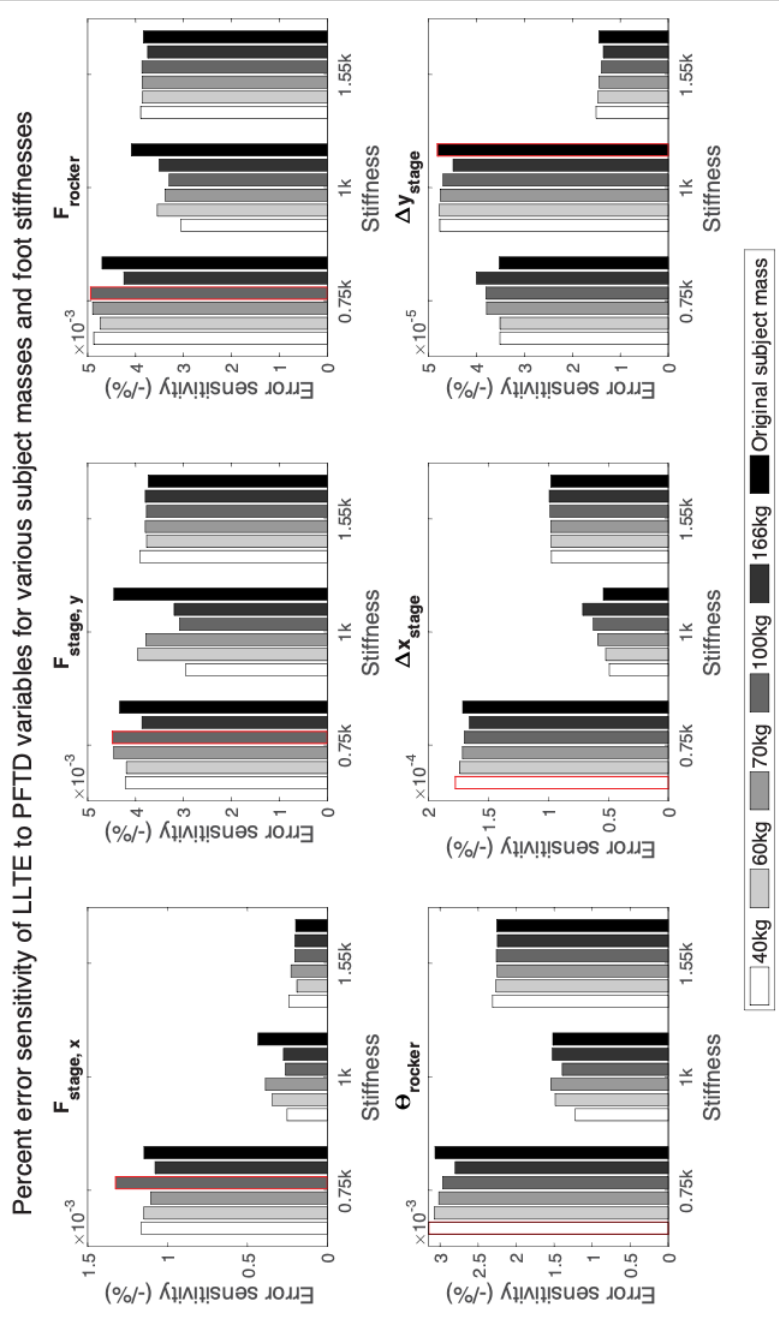
Figure A-2: Percent error sensitivity of LLTE to each PFTD variable for various subject mass and foot stiffness categories. The maximums off these values (outlined in red) are used as the percent error sensitivities.

Appendix B

Inherited Design

Prior to the work described in this thesis, a version of the PFTD was designed and partially constructed. Displayed in Fig. B-1, this inherited device was not capable of accurately measuring the LLTE values of the full range of commercially available feet, which prompted the redesign work that is the basis of this thesis.

Figure B-1 displays the architecture of the device, which was designed to be used in tandem with an Instron material testing machine (MTM). The device provided two degrees of actuation through a linear stage module and a rocker platform and the MTM provided the third degree of actuation. In the rocker platform of the inherited device, an AC brushless servo motor equipped with a gearbox actuated the rocker platform. A torque sensor situated in between the motor shaft and rocker platform axis measured the torque applied to the rocker platform, which was used to calculate the CoP. In the linear stage module, a stepper motor actuated the linear stage, which was mounted on top of the rocker platform. A load cell mounted in between the linear stage carriage and the foot platform measured the horizontal GRF applied to the foot. The base plate of the device was bolted to an MTM and the prosthetic foot was fastened to the MTM pylon, which was attached to the MTM load cell, which measured the vertical force applied to the foot in the global reference frame. Horizontal and rotational displacements were measured by the motor encoders in the stepper and servo motors, respectively, and vertical displacement was measured by the MTM.

There were several design elements of this device that rendered it incapable of testing the full commercial range of prosthetic feet. The inherited device was stated to have been designed to test feet that were suitable for subject masses up to 100 kg (compared with the PFTD, which is designed to test feet suited for subject masses up to 200 kg). Therefore, many of the components were incapable of supplying or measuring the loads that a 200 kg user experiences. The torque sensor, for example, was rated for a maximum capacity of 200 Nm, which is far less than the 724 Nm (including a safety factor) required to test a foot sized for a 200 kg user.

Due to several design choices and oversights, the inherited device was also incapable of measuring the LLTE value with a meaningful accuracy. The torque sensor, gearbox, and Instron MTM load cell all independently exceeded the total allowable error (LLTE accuracy requirement, Table 2.1) of the entire device. The torque sensor shafts were attached to the motor and rocker platform using keyways and set screws, which introduced additional error. The load cell in the linear stage module was installed directly between the stage carriage and the foot platform, which means it was being used to constrain the rotation of the stage carriage. This created an inappropriate moment equal to the full torque of the stepper motor, which introduced error and would ultimately damage the load cell. Similarly, the Instron MTM load cell was experiencing high off-axis loading that exceeded its rated capacity, which contributed to the error mentioned earlier and would ultimately damage the load cell. In addition, by being secured at the front and back ends (Fig. B-1b), the servo motor and gearbox were overconstrained, which could introduce error and damage the components. As a last example, the value of x_0 in the inherited design was arbitrarily set to 0.05 m, which is less optimal than the 0.085 m value used in the PFTD design. Section 4 discusses more of the alternate design elements included in the PFTD in contrast to the inherited design elements reviewed here.
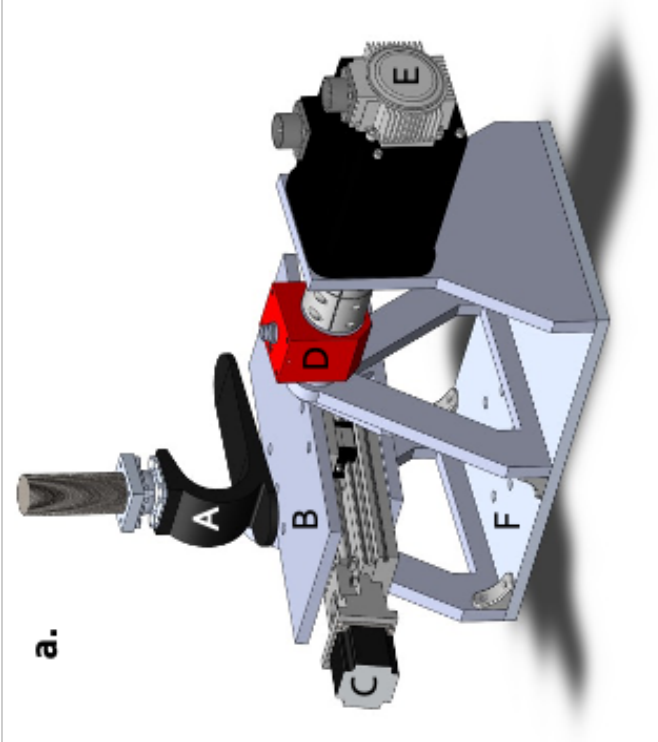
Figure B-1: Inherited device design. a) CAD image of the device and a prosthetic foot with several components labeled: foot (A), linear stage (B), stepper motor (C), torque sensor (D), servo motor and gearbox (E), base plate that rigidly attaches to an MTM (F). b) The realized device and a prosthetic foot mounted in an Instron MTM.

Bibliography

[1] Peter G. Adamczyk and Arthur D Kuo. Mechanical and energetic consequences of rolling foot shape in human walking. *The Journal of experimental biology*, 216(Pt 14):2722–31, 2013.

[2] Endolite North America. *Catalog 2016/17 – Lower limb prosthetic product range.* endolite.com, Miamisburg, OH, 2016.

[3] American Orthotic & Prosthetic Association. Aopa prosthetic foot project report. Technical report, sep 2010.

[4] Patrick M. Aubin, Matthew S. Cowley, and William R. Ledoux. Gait simulation via a 6-dof parallel robot with iterative learning control. *IEEE Transactions on Biomedical Engineering*, 55(3):1237–1240, 2008.

[5] Thirunindravur Mannan Balaramakrishnan, Sundararajan Natarajan, and Sujatha Srinivasan. Roll-over shape of a prosthetic foot: a finite element evaluation and experimental validation. *Medical and Biological Engineering and Computing*, 58:2259–2270, 2020.

[6] Carolin Curtze, At L. Hof, Helco G. van Keeken, Jan P.K. Halbertsma, Klaas Postema, and Bert Otten. Comparative roll-over analysis of prosthetic feet. *Journal of Biomechanics*, 42(11):1746–1753, 2009.

[7] Larry L. Howell (Editor), Spencer P. Magleby (Editor), and Brian M. Olsen (Editor). *Handbook of Compliant Mechanisms*, chapter 12, pages 193–276. John Wiley & Sons, Ltd, 2013.

[8] Fillauer. *Lower Extremity Prosthetics Product Catalog.* www.fillauer.com, Chattanooga, TN, jun 2020.

[9] Robert Gailey, Kerry Allen, Julie Castles, Jennifer Kucharik, and Mariah Roeder. Review of secondary physical conditions associated with lower-limb amputation and long-term prosthesis use. *Journal of rehabilitation research and development*, 45(1):15–29, 2008.

[10] Mark D. Geil. An iterative method for viscoelastic modeling of prosthetic feet. *Journal of Biomechanics*, 35(10):1405–1410, 2002.

[11] Brian J. Hafner. Clinical Prescription and Use of Prosthetic Foot and Ankle Mechanisms: A Review of the Literature. *Journal of Prosthetics and Orthotics*, 17(Supplement):S5–S11, 2005.

[12] Brian J Hafner, Joan E Sanders, Joseph Czerniecki, and John Fergason. Energy storage and return prostheses: does patient perception correlate with biomechanical analysis? *Clinical Biomechanics*, 17(5):325–344, 2002.

[13] Andrew H. Hansen, D S Childress, and E H Knox. Prosthetic foot roll-over shapes with implications for alignment of trans-tibial prostheses. *Prosthetics and Orthotics International*, 24(3):205–215, jan 2000.

[14] Cheriel J Hofstad, H Linde, J Limbeek, and Klaas Postema. Prescription of prosthetic ankle-foot mechanisms after lower limb amputation. *The Cochrane database of systematic reviews*, 2010(1):CD003978, 2004.

[15] Freedom Innovations. *Lower Limb Prosthetic Solutions Product Catalog.* www.freedom-innovations.com, Irvine, CA, 2015.

[16] ISO Central Secretary. Prosthetics — structural testing of lower-limb prostheses — requirements and test methods. Standard ISO 10328:2016, International Organization for Standardization, Geneva, CH, 2016.

[17] ISO Central Secretary. Prosthetics — testing of ankle-foot devices and foot units — requirements and test methods. Standard ISO 22675:2016, International Organization for Standardization, Geneva, CH, 2016.

[18] W. Brett Johnson, Victor Prost, Pooja Mukul, and V. Amos G. Winter. Design and Evaluation of High-Performance, Low-Cost Prosthetic Feet for Developing Countries. *Journal of Biomechanical Engineering (In Review)*, 2021.

[19] David E Krebs, Joan E Edelstein, and Maureen A Thornby. Prosthetic Management of Children with Limb Deficiencies. *Physical Therapy*, 71(12):920–934, 12 1991.

[20] Erik P. Lamers, Maura E. Eveld, and Karl E. Zelik. Subject-specific responses to an adaptive ankle prosthesis during incline walking. *Journal of Biomechanics*, 95:109273, 2019.

[21] J F Lehmann, R Price, S Boswell-Bessette, A Dralle, K Questad, and B J De-Lateur. Comprehensive analysis of energy storing prosthetic feet: Flex foot and seattle foot versus standard sach foot. *Archives of Physical Medicine & Rehabilitation*, 74(11):1225–1231, 1993.

[22] Harmen Van Der Linde, Cheriel J Hofstad, Alexander C H Geurts, Klaas Postema, Jan H B Geertzen, and Jacques van Limbeek. A systematic literature review of the effect of different prosthetic components on human functioning with a lower-limb prosthesis. *Journal Of Rehabilitation Research And Development*, 41(4):555–570, 2004.

[23] Matthew J. Major and Nicholas P. Fey. Considering passive mechanical properties and patient user motor performance in lower limb prosthesis design optimization to enhance rehabilitation outcomes. *Physical Therapy Reviews*, 22(3-4):202–216, 2017.

[24] Matthew J. Major, Laurence P.J. Kenney, Martin Twiste, and David Howard. Stance phase mechanical characterization of transtibial prostheses distal to the socket: A review, 2012.

[25] Kathryn Olesnavage, Victor Prost, Brett Johnson, Matthew Major, and Amos G. Winter. Experimental Demonstration of the Lower Leg Trajectory Error Framework Using Physiological Data as Input. *Journal of Biomechanical Engineering*, 143(March), 2020.

[26] Kathryn M. Olesnavage, Victor Prost, William Brett Johnson, and V. G. Amos Winter. Passive prosthetic foot shape and size optimization using lower leg trajectory error. *Journal of Mechanical Design, Transactions of the ASME*, 140(10), 2018.

[27] Kathryn M. Olesnavage and Amos G. Winter. A Novel Framework for Quantitatively Connecting the Mechanical Design of Passive Prosthetic Feet to Lower Leg Trajectory. *IEEE Transactions on Neural Systems and Rehabilitation Engineering*, 26(8):1544–1555, 2018.

[28] World Health Organization et al. *World report on disability 2011.* World Health Organization, 2011.

[29] Ossur. *Prosthetic Solutions Catalogue.* www.ossur.com, Reykjavik, Iceland, 2016.

[30] Ottobock. *Prosthetics – Lower limbs.* www.ottobock.com, Duderstadt, Germany, 2015.

[31] Nicola Petrone, Gianfabio Costa, Gianmario Foscan, Francesco Bettella, Gianluca Migliore, and Andrea Giovanni Cutti. Conceptual design of a new multicomponent test bench for the dynamic characterization of running specific prostheses. *Proceedings*, 49(1), 2020.

[32] Klaas Postema, H J Hemens, J De Vries, H. F.J.M. J Koopman, and W. H. Eisma. Energy storage and release of prosthetic feet part 1: biomechanical analysis related to user benefits. *Prosthetics and Orthotics International*, 21:17–27, 1997.

[33] Mark A. Price, Philipp Beckerle, and Frank C. Sup. Design Optimization in Lower Limb Prostheses: A Review. *IEEE Transactions on Neural Systems and Rehabilitation Engineering*, 27(8):1574–1588, jul 2019.

[34] V. Prost, W. B. Johnson, J. A. Kent, M. J. Major, and V. A. G. Winter. Sensitivity investigation of the lower leg trajectory error framework and its implication

for the design and evaluation of ankle-foot prostheses. *Journal of Biomechanical Engineering (In Progress)*, 2021.

[35] Victor Prost, W. Brett Johnson, Jenny A. Kent, Matthew J. Major, and V. Amos G. Winter. Biomechanical evaluation of prosthetic feet designed using the Lower Leg Trajectory Error framework. *Scientific Reports (In Review)*, 2021.

[36] Victor Prost, Kathryn M. Olesnavage, W. Brett Johnson, Matthew J. Major, and V. Amos G. Winter. Design and testing of a prosthetic foot with interchangeable custom springs for evaluating lower leg trajectory error, an optimization metric for prosthetic feet. *Journal of Mechanisms and Robotics*, 10(2):1–8, 2018.

[37] Billie J. Randolph, Leif M. Nelson, and M. Jason Highsmith. A review of unique considerations for female veterans with amputation. *Military Medicine*, 181(S4):66–68, 11 2016.

[38] R.J. Roark, W. Young, R. Budynas, and Y. Warren. *Roark's Formulas for Stress and Strain.* McGraw Hill professional. Mcgraw-hill, seventh edition, 2002.

[39] M. Sam, A.H. Hansen, and D.S. Childress. Mechanical characterization of prosthetic feet using a prosthetic foot loading apparatus. In *Proceedings of the 22nd Annual International Conference of the IEEE Engineering in Medicine and Biology Society (Cat. No.00CH37143)*, volume 3, pages 1968–1971, Chicago, 2000. IEEE.

[40] Elisabeth Schaffalitzky, Pamela Gallagher, Malcolm MacLachlan, and Stephen T. Wegener. Developing consensus on important factors associated with lower limb prosthetic prescription and use. *Disability and Rehabilitation*, 34(24):2085–2094, 2012.

[41] Max K Shepherd, Alejandro F Azocar, Matthew J Major, and Elliott J Rouse. Amputee perception of prosthetic ankle stiffness during locomotion. *Journal of NeuroEngineering and Rehabilitation*, 15(1), 2018.

[42] Max K. Shepherd and Elliott J. Rouse. Comparing preference of ankle–foot stiffness in below-knee amputees and prosthetists. *Scientific Reports*, 10(1), 2020.

[43] S. L. Toh, J. C.H. Goh, P. H. Tan, and T. E. Tay. Fatigue testing of energy storing prosthetic feet. *Prosthetics and Orthotics International*, 17(3):180–188, 1993.

[44] H. W.L. L. Van Jaarsveld, H. J. Grootenboer, H. F.J.M. J. M. Koopman, J. De Vries, and H. F.J.M. J. M. Koopman. Stiffness and hysteresis properties of some prosthetic feet. *Prosthetics and Orthotics International*, 14(3):117–124, 1990.

[45] Andrea B. Wanamaker, Rebecca R. Andridge, and Ajit M.W. Chaudhari. When to biomechanically examine a lower-limb amputee: A systematic review of accommodation times. *Prosthetics and Orthotics International*, 41(5):431–445, 2017.

[46] Christina M. Webber and Kenton Kaufman. Instantaneous stiffness and hysteresis of dynamic elastic response prosthetic feet. *Prosthetics and Orthotics International*, 41(5):463–468, 2017.

[47] David A Winter. *Biomechanics and motor control of human movement*. John Wiley & Sons, 2009.

[48] Xueyi Zhang, Goeran Fiedler, and Zhicheng Liu. Evaluation of gait variable change over time as transtibial amputees adapt to a new prosthesis foot. *BioMed Research International*, 2019(i), 2019.

[49] Kathryn Ziegler-Graham, EJ Ellen J. MacKenzie, Patti L. PL Ephraim, Thomas G. Travison, and Ron Brookmeyer. Estimating the prevalence of limb loss in the United States: 2005 to 2050. *Archives of physical medicine and rehabilitation*, 89(3):422–9, 2008.